

Kinematics of the Galactic Halo from Horizontal Branch stars in the Hamburg/ESO Survey

Christopher Thom^{1,2}, Chris Flynn², Michael S. Bessell³, Jyrki Hänninen², Timothy C. Beers⁴, Norbert Christlieb⁵, Dionne James⁶, Johan Holmberg², Brad K. Gibson¹

¹ *Astrophysics and Supercomputing Centre, Swinburne University, Melbourne, Australia*

² *Tuorla Observatory, Väisäläntie 20, FI-21500, Piikkiö, Finland*

³ *Mt Stromlo and Siding Spring Observatory, ANU, Canberra, Australia*

⁴ *Department of Physics & Astronomy, and JINA: Joint Institute for Nuclear Astrophysics, Michigan State University, E. Lansing, MI, 48824, USA*

⁵ *Hamburger Sternwarte, Gojenbergsweg 112, D-21029, Hamburg, Germany*

⁶ *Anglo-Australian Observatory, PO Box 296, Epping, NSW 1710, Australia*

Accepted Received ; in original form

ABSTRACT

Large samples of Field Horizontal Branch (FHB) stars make excellent tracers of the Galactic halo; by studying their kinematics, one can infer important physical properties of our Galaxy. Here we present the results of a medium-resolution spectroscopic survey of 530 FHB stars selected from the Hamburg/ESO survey. The stars have a mean distance of ~ 7 kpc and thus probe the inner parts of the Milky Way halo. We measure radial velocities from the spectra in order to test the model of Sommer-Larsen et al., who suggested that the velocity ellipsoid of the halo changes from radially-dominated orbits to tangentially-dominated orbits as one proceeds from the inner to the outer halo. We find that the present data are unable to discriminate between this model and a more simple isothermal ellipsoid; we suggest that additional observations towards the Galactic centre might help to differentiate them.

Key words: stars: horizontal branch – Galaxy: halo – Galaxy: kinematics and dynamics

1 INTRODUCTION

The stellar halo only comprises about 1% of the luminous mass of the Galaxy and is composed of very old, metal-poor stars. In spite of this, the present-day dynamical and chemical state of the stellar halo has exerted considerable influence in shaping our understanding of the formation of large disk galaxies such as the Milky Way, particularly in its very early stages.

Large samples of Field Horizontal Branch stars (FHBs) in the Galactic halo are excellent “test particles” for studies of halo kinematics (e.g. Sommer-Larsen et al. 1994, 1997; Sirko et al. 2004a); tracing the mass (Beers et al. 2004) and the merger history (Kinman et al. 1994; Brown et al. 2004) of the Milky Way. Their intrinsic brightness and the relative ease with which distances can be obtained, together with their relatively clean spectra, also make them ideal probes of distances to High Velocity Clouds (e.g. Schwarz et al. 1995; Thom et al., in preparation).

The HK survey of Beers and collaborators (e.g.

Beers et al. 1985, 1992) has identified $\sim 12,000$ candidate Horizontal Branch stars, of which about half are expected to be on the Horizontal Branch; the other half appear to be a mixture of A-type main-sequence stars and halo blue stragglers (Beers et al. 1988, 1996). More recently, several groups have reported large and clean samples of Horizontal Branch stars. The Hamburg/ESO survey (HES), originally designed to identify low-luminosity quasars, has been shown to contain a remarkable sample of interesting stars, including 8321 FHBs. This sample has a contamination level by non-FHBs (mostly high-gravity A-type stars) of less than 16% (Christlieb et al. 2004). A subset of these stars is used here to constrain models of halo kinematics.

The Sloan Digital Sky Survey (SDSS), although primarily designed for extragalactic studies, has also revealed a large sample of 1170 Horizontal Branch stars at distances up to ~ 100 kpc (Sirko et al. 2004b). From this sample Sirko et al. (2004a) measured an isotropic velocity ellipsoid for the outer halo. This result contrasts with halo stars in the solar neighbourhood, which show an ellipsoid elongated

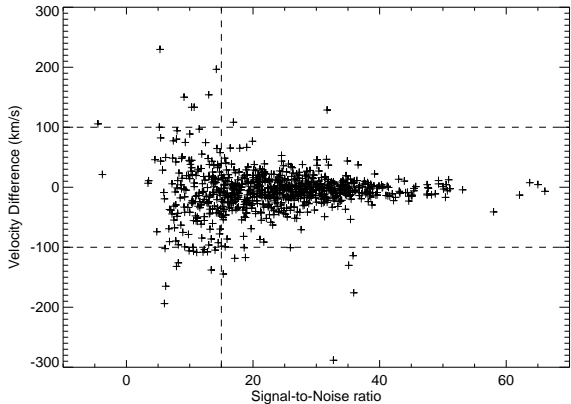


Figure 1. Radial velocity differences, as measured using the $H\delta$ and $H\gamma$ lines, versus Signal-to-Noise ratio of the spectra, for our sample stars. The vertical and horizontal lines indicate the adopted $S/N > 15$ and $|v_{\text{diff}}| < 100 \text{ km s}^{-1}$ limits, respectively (see text).

in the radial direction (Chiba & Beers 2000; Gould 2003, 2004).

Wilhelm et al. (1999) have described a technique for separating Horizontal Branch stars from higher gravity A stars on the basis of broadband UBV colours and medium-resolution spectroscopy. Clewley et al. (2002, 2004) explored similar techniques based on broadband colours and medium-resolution spectroscopy, and also presented a method relying solely on medium resolution spectroscopy. They used this method to identify ~ 100 stars at distances of > 30 kpc with the aim of providing better constraints on the mass of the Milky Way.

Brown et al. (2004) used the full *2MASS* point-source catalogue to select close to 100,000 objects, of which they expect 47% to be on the Blue Horizontal Branch. They find an absence of structure in the inner halo (the sample has distance $d < 9$ kpc), concluding that there have been no major accretion events in the inner halo over the past few Gyrs.

Here we present the results of a programme to obtain radial velocities (RVs), and study the kinematics, of more than 500 FHB stars selected from the HES catalogue. We wish to test specifically the predictions of the Sommer-Larsen et al. (1994) (hereafter, SLFC) model, as refined by Sommer-Larsen et al. (1997). In the SLFC model, the velocity ellipsoid of the halo changes from radially-dominated orbits to tangentially-dominated orbits as one proceeds from the inner to the outer halo. We attempt to distinguish between this model and the simpler isothermal halo model, which specifies an isotropic distribution of stellar orbits, independent of Galactocentric radius, in the outer halo. Section 2 presents the sample and observations. It also includes details on the radial velocity measurements and selection criteria. Section 3 discusses the models which we wish to test. Section 4 details the final sample selection, division into fields, and calculation of the line-of-sight velocity dispersions, σ_{LOS} . Section 5 presents the major results and analysis. A summary and conclusions are provided in Section 6.

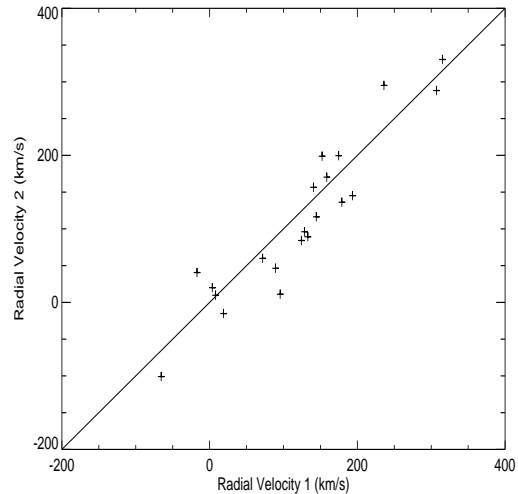


Figure 2. RV1 versus RV2 for the 21 stars with repeated measurements. The solid line is the one-to-one correspondence.

2 SAMPLE AND OBSERVATIONS

Our sample of stars was drawn from the Christlieb et al. (2004) catalogue of FHB stars selected from the Hamburg/ESO survey. As part of a large programme of follow-up observations of the stellar content of the HES and HK surveys, over 1100 FHB stars were observed at the UK Schmidt Telescope (UKST)¹, using the six degree fibre-fed spectrograph. The 6dF instrument allows one to observe up to 150 objects simultaneously across the 6° field of the Schmidt telescope, obtaining spectra at 2 \AA resolution. More than forty nights of observations took place between April 2001 and April 2003. Integration times were typically 4–5 times 2700 s per field, depending on observing conditions.

The targets were, in most cases, selected by HES field number, with roughly equal numbers of fibres used for metal-poor candidates and FHB stars. The data were reduced using the *Figaro* and *6dfdr* software packages, the latter being written specifically to handle the fibre data from the 6dF instrument. This process yielded *FITS* files containing the reduced spectra of all 150 fibres. These files were separated, with one spectrum per file and assigned a unique name based on the star name, field number, and date of observation. A hand-screening process was then used to exclude obvious problems and artefacts.

Catalogues of FHB stars may contain a significant fraction of contaminants – higher surface gravity A-type stars which fall within the colour range of the survey (in the case of the HES, $-0.2 < B - V < 0.3$). Since the HES FHB candidates have been shown to have a much lower level of contamination from higher-gravity stars ($< 16\%$; Christlieb et al. 2004), as compared to the HK survey ($\sim 50\%$; Beers et al. 1996), we considered only the HES stars in our observations. We made no attempt to separate the potential contaminants from the true FHB stars, judging that a $\sim 16\%$ level is ac-

¹ The UKST is operated and supported by the Anglo-Australian Observatory, on behalf of the astronomical communities of Australia and the UK

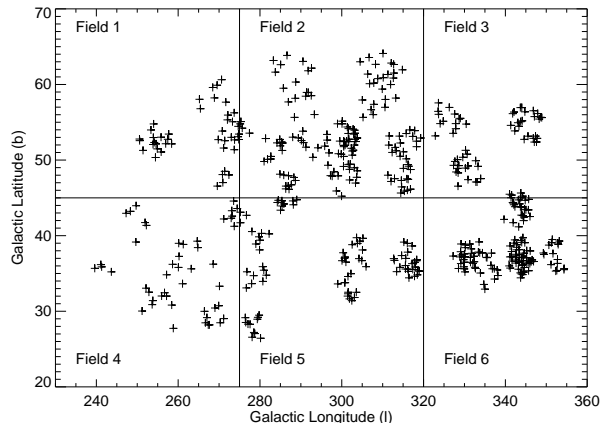


Figure 3. Sky distribution of all 530 stars in 6 northern fields.

ceptable for our present purpose. While it is, in principle, possible to further refine the classification, using the spectroscopic method of Clewley et al. (2002) would result in a sample clean to about the $\sim 12\%$ level and hence nothing would be gained. Since systematic, accurate photometry is not available, methods based on this are not applicable. Conversely, we have no way of obtaining RVs from the objective prism of the HES, but can measure velocities in the 6df spectra, since the S/N requirements for RVs are less stringent than those for classification.

2.1 Radial Velocities and Selection

Sersic profiles were fit to the $H\gamma$ and $H\delta$ Balmer lines, as described by Clewley et al. (2002). Due to changes in the spectrograph settings over the long observing period, these were the only two prominent lines common to all spectra. We rejected any star for which we could not obtain a radial velocity measurement in both lines. We also noticed large systematic discrepancies ($> 150 \text{ km s}^{-1}$) between the measurements of RV from the $H\gamma$ and $H\delta$ lines in some stars. These stars were noted to be concentrated in one field (HES field 573), hence all stars in this field were rejected. One star was also rejected due to difficulties with sky subtraction. This left a total of 827 stars.

We sought to combine the velocity measurements from the two lines into an average value, but we first used the difference in the measurements of the two lines to provide an internal consistency check on the radial velocities. Fig. 1 shows a plot of the difference between the $H\delta$ and $H\gamma$ line, versus signal-to-noise ratio. We applied cuts, retaining all stars with measurement difference less than 100 km s^{-1} and S/N greater than 15, as shown in Fig 1. An average RV was then computed from all available measurements. Heliocentric corrections were calculated using the IRAF task *rvcorrect*. This selection yielded 636 RV measurements.

Twenty-one stars in our sample were observed at more than a single epoch and thus enable a further check on the measurements. The correlation between the two average RVs for these stars is shown in Fig. 2. The difference between these two measurements for a given star – the range of measurements – provides an estimate of the standard deviation of the underlying error distribution (Pearson 1926; Tippett

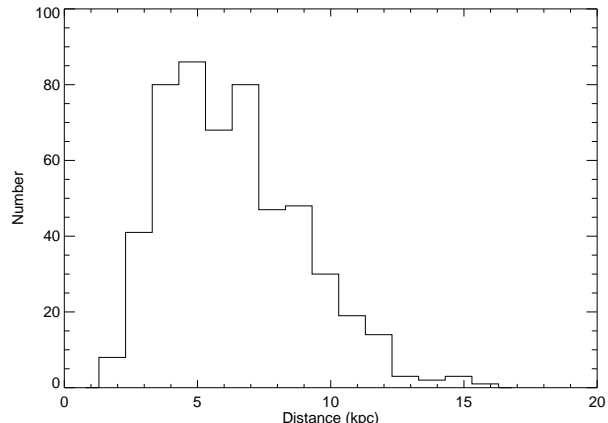


Figure 4. Histogram of heliocentric distances for the final sample of 530 stars.

1925). This distribution will be normally distributed with $\mu = RV$ and $\sigma = \text{error in the measurement}$. Applying a correction factor of 1.12838 (see Table X of Tippett 1925) to the absolute value of the range, we obtain a mean statistical velocity error of 30 km s^{-1} . This agrees well with the assumption of Gaussian errors, under which we obtain 27 km s^{-1} , dividing the standard deviation of the velocity differences by $\sqrt{2}$. We therefore adopt 30 km s^{-1} as the formal error on our radial velocity measurements. To definitively characterise the error on a single RV measurement would require many repeated velocity measurements of the same star. For the analysis, the two RV measurements were combined into a single entry by averaging the two independent RVs, weighted by the S/N in the respective spectra, yielding RVs for 615 unique stars.

3 KINEMATIC MODELS

The density distribution of the stellar halo follows a power-law, $R^{-\alpha}$, with Galactocentric radius, R . The value of α has been the subject of many studies, using RR Lyrae stars, halo giants, and Blue Horizontal Branch (BHB) stars (e.g. Preston et al. 1991; Kinman et al. 1994; Sluis & Arnold 1998; Morrison et al. 2000). Most of these converge on a value of $\alpha \approx 3.0 - 3.5$. In contrast, Robin et al. (2000) find a lower value consistent with the range $\alpha = 2.0 - 2.75$, whilst noting significant degeneracy between α and the flattening parameter c/a . This contrasts with the density distribution of the Galactic dark halo, which follows R^{-2} (i.e., the isothermal case expected from a flat rotation curve), at least in the outer parts where it dominates over the luminous matter.

Stars in the halo of the Milky Way are drawn from a population with a total dispersion on the order of 200 km s^{-1} , i.e. they have velocities needed to maintain equilibrium with the Galactic gravitational potential. In the stellar halo, this velocity is directed roughly equally into three components, resulting in a system with little bulk rotation and thus mainly “pressure support” against gravitational collapse.

The three components of the stellar halo’s velocity ellipsoid have been measured accurately in the solar neigh-

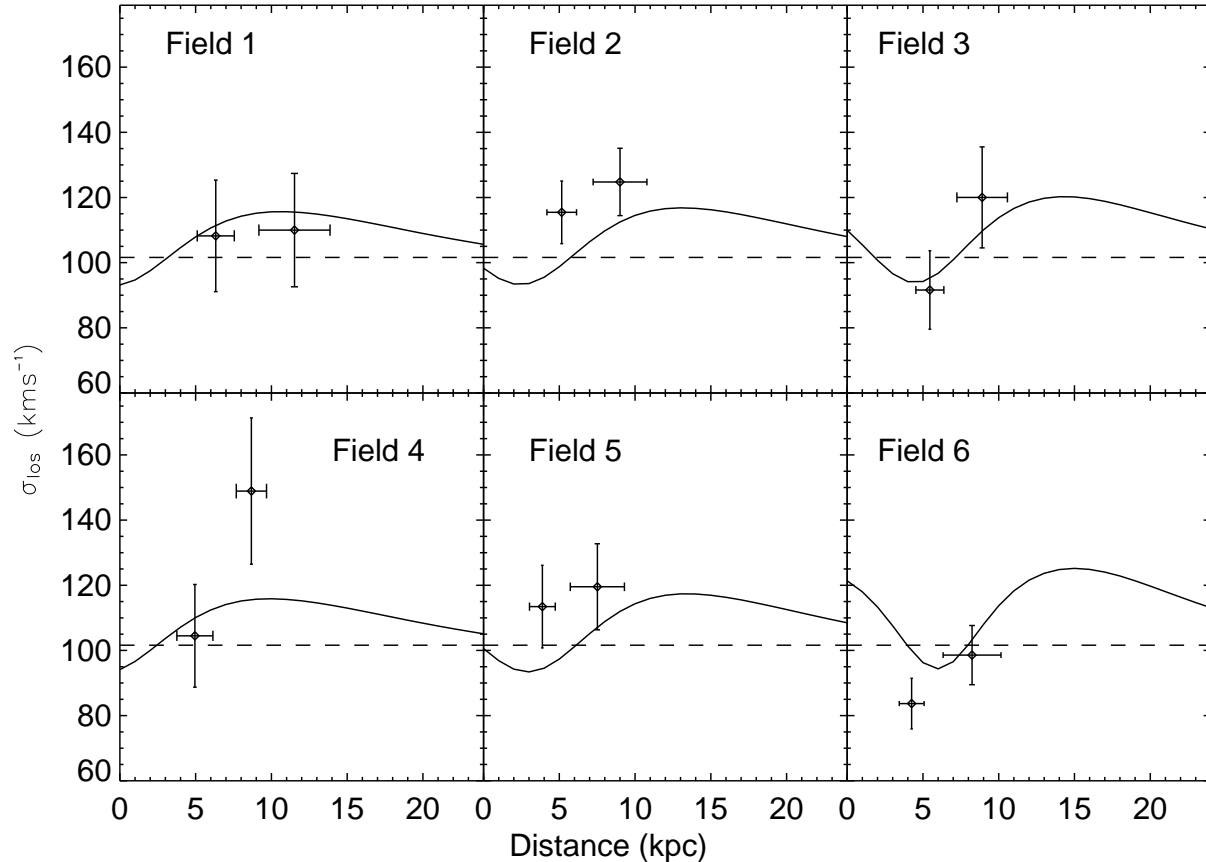


Figure 5. Comparison of measured σ_{LOS} to the two models. The horizontal dashed line shows an isothermal model with the value measured by Sirko et al.. The solid line is the line-of-sight velocity dispersion predicted by the SLFC model for the average line-of-sight of the field. The error bars show the 1σ errors.

bourhood, for stars within roughly 1 kpc of the Sun, to be $\sigma = (\sigma_R, \sigma_\theta, \sigma_\phi) \approx (140, 100, 100) \text{ km s}^{-1}$ (Chiba & Beers 2000; Gould 2003), where we have adopted a spherical coordinate system (R, θ, ϕ) around the Galactic centre. This determination is based on stars for which all three components of the space velocity can be measured via both radial line-of-sight velocities and proper motions. Beyond a few kpc from the Sun, usually only the radial velocity can be measured (a situation which will change dramatically when the ESA GAIA mission is completed; Perryman 2002), and special techniques are required to reconstruct the three components of the velocity ellipsoid. One can either propose and fit data to models of the velocity ellipsoid as a function of position in the Galaxy – as performed by Sommer-Larsen et al. (1997) for some ~ 700 stars – or attempt to recover the three components directly (Sirko et al. 2004a).

The velocity ellipsoid of the stellar halo is a consequence of its density profile and the total matter distribution in the Galaxy. Let us assume that the 3-D dispersion of the velocity distribution is isothermal (i.e., it has the same magnitude in all three components), and that the density falls off like $R^{-\alpha}$. It then follows, for a Galactic potential dominated by a dark halo with a flat rotation curve (characterised by constant circular velocity V_0) that $\sigma = V_0/\sqrt{\alpha}$. For the Milky Way, $V_0 \approx 220 \text{ km s}^{-1}$, and thus $\sigma \approx 120 \text{ km s}^{-1}$ for each

component (Binney & Tremaine 1987). The total velocity dispersion is then of order $\sqrt{3}\sigma \approx 200 \text{ km s}^{-1}$.

The stellar halo is clearly not isothermal in the vicinity of the Sun (the component of the velocity dispersion in the radial direction is $\approx 40\%$ larger than the two other components of the velocity ellipsoid); nevertheless, the total velocity dispersion is of order 200 km s^{-1} .

What is the velocity dispersion like elsewhere in the halo? SLFC and Sirko et al. (2004a) have attempted a reconstruction from radial velocities of distant halo stars. SLFC proposed a model for the velocity dispersion $\sigma(R, \theta, \phi)$ as a function of Galactocentric radius R alone; the model permitted sharp deviations from isothermal behaviour (such as is seen in the solar neighbourhood) and was fit to both the local and distant halo stars. This model was subsequently refined using a much larger sample of about ~ 700 distant halo stars by Sommer-Larsen et al. (1997). It was found that the radial anisotropy ($\sigma_R > \sigma_{\phi, \theta}$) seen near the Sun persists into the inner halo ($R < 8 \text{ kpc}$), changing to tangential anisotropy in the outer halo (roughly $R > 15 - 20 \text{ kpc}$). Sirko et al. (2004a) present an ostensibly opposing view; from radial velocities of 1170 halo stars found in the SDSS, they found that the velocities of (distant) halo stars are very close indeed to isothermal ($(\sigma_R, \sigma_\theta, \sigma_\phi) = (101.4 \pm 2.8, 97.7 \pm 16.4, 107.4 \pm 16.6) \text{ km s}^{-1}$). The Sirko et al. study is essentially of the outer halo, where

the SLFC model is not yet well constrained, hence the ostensible contradiction with the non-isothermal model of SLFC is, as those authors argued, probably not significant.

We treat the halo’s kinematics statistically, characterised by the velocity ellipsoid alone; i.e. we explicitly ignore substructure, such as dissolving satellites or other features in density and/or velocity space. From the point of view of halo substructure, the halo can be divided into inner and outer regions. The inner halo is that part which is within ~ 15 kpc radius from the Galactic centre. In this region, the relevant dynamical time scales are expected to be considerably shorter than the age of the Galaxy. This expectation is borne out by the lack of detected substructure (e.g. Brown et al. 2004). Thus, in the inner halo, the stellar population appears likely to be fairly well mixed, with a smooth density distribution. There is additional evidence that this is the case in the solar neighbourhood, based on an analysis of 4588 sub-dwarfs (Gould 2003, 2004). In the outer halo, beyond some 20 kpc or so, dynamical time scales approach the age of the Galaxy. In these regions it has long been suspected that the halo would contain the debris of dissolving satellite galaxies; this is now well established (e.g. Majewski 1994; Ibata et al. 1994; Lynden-Bell & Lynden-Bell 1995; Morrison et al. 2000). While the outer halo is undoubtedly quite lumpy, most of the stellar halo’s mass, and most of that part probed via our data, is in the well mixed inner halo. Additional tests of this assertion will be the subject of a forthcoming study.

4 FINAL SAMPLE AND VELOCITY DISPERSION

We analysed the kinematics of our stars following the methodology of SLFC. This involved dividing the sample into regions on the sky in which there are sufficient stars to measure σ_{LOS} for two distance bins along the line of sight. The stars in each field were split evenly into the two distance bins. The requirement we applied, that each bin should have at least twenty stars, forced us to exclude all stars with Galactic latitude $b < 0^\circ$. This left us with a total of 530 stars with which to study the kinematics of the Galactic halo. The distribution on the sky of all 530 FHB stars in our final sample is shown in Fig. 3. The average distance to the stars is 6.7 kpc; the distance distribution is shown in Fig 4.

In calculating the velocity dispersion along the line-of-sight (σ_{LOS}) we excluded the upper and lower 5% the data, in order to protect these numbers from the adverse effects of outliers. The result is adjusted by a factor of $\frac{1}{0.789}$ to recover the true standard deviation of the original distribution, a process described in detail by Morrison et al. (1990). The σ_{LOS} were corrected for a 30 km s^{-1} velocity measurement error by subtraction in quadrature and then compared to the model predictions. We have consistently used velocities in a heliocentric frame throughout the calculations, with the corresponding distance. Since the model predictions are made in a galactocentric frame, a projection factor was applied to recover the appropriate line-of-sight value.

Table 1. Definition of fields in Galactic co-ordinates, showing Bottom Left Corner (BLC), Top Right Corner (TRC), number of stars, distance and σ_{LOS} of stars in field. Errors are 1σ .

Field	BLC (l, b)	TRC (l, b)	Num	Dist (kpc)	σ_{LOS} km s^{-1}
Field 1	(220,45)	(275,70)	22	6.3 ± 1.2	108 ± 17
			22	11.5 ± 2.3	110 ± 17
Field 2	(275,45)	(320,70)	78	5.2 ± 1.0	115 ± 10
			79	9.0 ± 1.8	125 ± 10
Field 3	(320,45)	(360,70)	31	5.5 ± 0.9	92 ± 12
			32	8.9 ± 1.7	120 ± 15
Field 4	(220,20)	(275,45)	24	5.0 ± 1.2	104 ± 16
			24	8.7 ± 1.0	149 ± 22
Field 5	(275,20)	(320,45)	44	3.9 ± 0.8	113 ± 13
			45	7.5 ± 1.8	120 ± 13
Field 6	(320,20)	(360,45)	64	4.3 ± 0.8	84 ± 8
			65	8.2 ± 1.9	98 ± 9

5 RESULTS AND ANALYSIS

Table 1, in addition to listing the fields, shows the observed velocity dispersions and the $1\text{-}\sigma$ errors. These have been used to test both an isothermal, isotropic halo with velocity dispersion of 101.6 km s^{-1} (i.e., the value observed by Sirko et al. (2004a)) and the predictions of the SLFC model. Fig 5 shows this comparison for all six northern fields. The SLFC predictions are shown as the solid line, while the isothermal model is the horizontal dashed line. Visual inspection leads us to conclude that both models fit the data equally well; a χ^2 analysis confirms this view. Both models arise from predictions rather than fits to the data, and hence have no free parameters. For the twelve σ_{LOS} in the six fields we measured a reduced χ^2 of 1.31 and 1.85 for the SLFC and isothermal models respectively, with 12 degrees of freedom each. Since this is not a statistically significant difference, both must be regarded as fitting the data equally well.

5.1 Outer Halo Comparison

Sirko et al. (2004b) have provided a similar sample of 1170 FHB stars in the outer halo (distances up to ~ 100 kpc). From this sample they derive an estimate of the isothermal velocity dispersion of 101.6 km s^{-1} . We have analysed their data in the same manner as above (see their Table 3 for distances and heliocentric red-shift). The results are shown in Fig 6. At the distance of the Sirko data, both models predict similar line-of-sight velocity dispersions. Therefore these data are not an effective test of the SLFC model. These data, divided into nine fields and three distance bins per field, fit both models equally well. The reduced χ^2 statistics for the two models are 2.37 and 2.19 for the SLFC and isothermal models respectively, for 35 degrees of freedom, excluding the obvious outlier in panel 3 (third from left, top row in Fig 6). This data point is likely caused by the Sagittarius stream (Ibata et al. 1994), as noted by Sirko et al.. Again, the difference in χ^2 is not statistically significant.

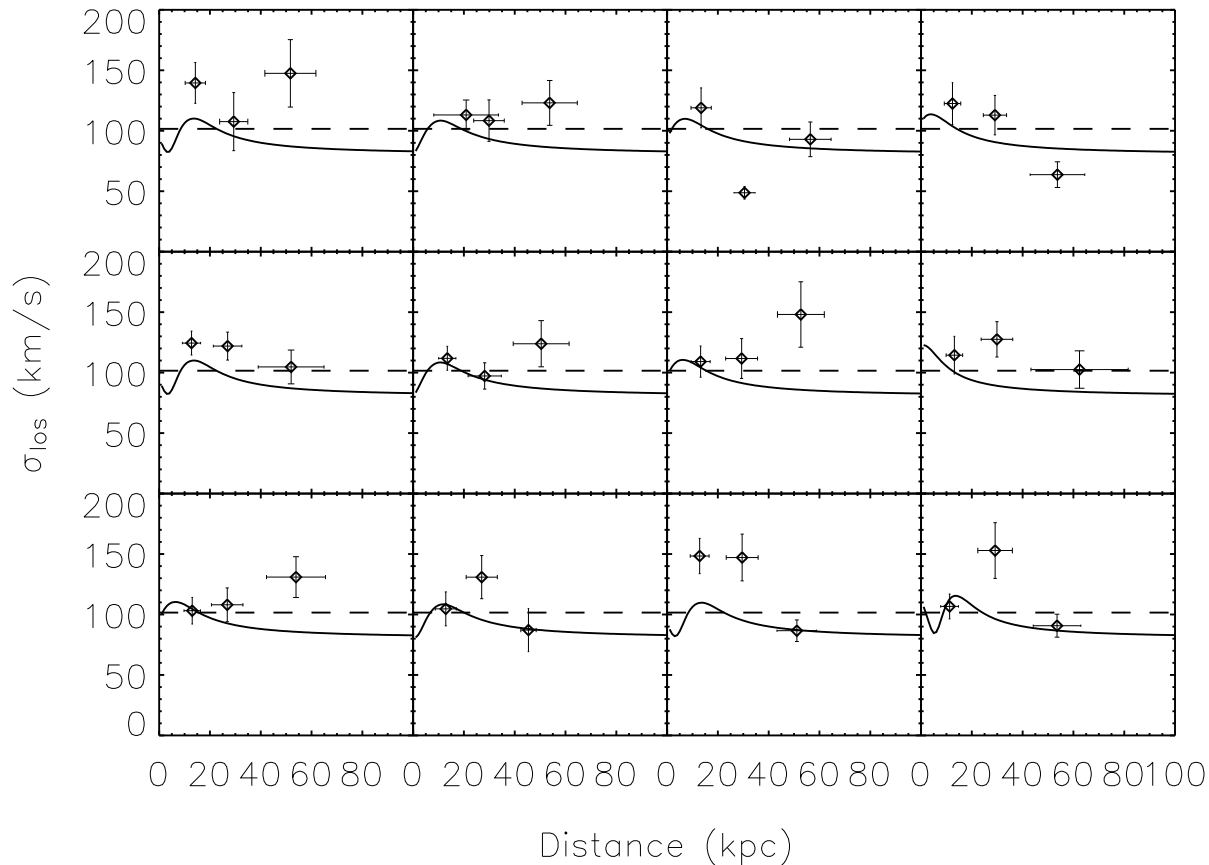


Figure 6. Comparison of Sirko et al. (2004b) data σ_{LOS} to the models fit by Sirko et al. (dashed lines) and SLFC (solid lines). Velocities are heliocentric and distances are in kpc.

5.2 Discussion

It is clear that neither this sample of inner Galactic halo stars, nor the outer halo sample of Sirko et al. (2004b), permit us to distinguish between the two competing models. It is worth noting here that the SLFC model is a physically realisable system (Flynn et al. 1996), whereas the isothermal model does not account for the locally observed halo velocity dispersion anisotropy. Where then should we look in order to best discriminate between these two models?

We have used the model of SLFC to determine regions on the sky where the two models differ in their predictions of σ_{LOS} by more than 30 km s^{-1} . This area is restricted to lines-of-sight toward the Galactic centre and at low Galactic latitude. Along these lines of sight one might expect a clear signature of the SLFC model, as demonstrated in Fig 7. A survey of 500 FHB stars at $(l, b) = (340 \text{ to } 20; -30 \text{ to } +30)$ with distance bins centred at 4, 8 and 13 kpc would provide a good discriminant between the models. This effect may also be seen in Field 6 of Fig 5, which is the closest the bulge.

6 SUMMARY AND CONCLUSIONS

Line of sight velocities have been measured for a sample of 530 FHB stars in the inner Galactic halo, with

an average heliocentric distance of 6.7 kpc. We have used these velocities to test the velocity dispersions predicted by the Sommer-Larsen et al. (1994) halo model, and compared with those predicted by an isothermal model. The former model allows for marked anisotropies to account for the well-constrained parameters of the local Galactic halo. These new data are equally well described by both models. We also compared the model predictions to the sample of 1170 FHB stars in the outer Galactic halo, as published by Sirko et al. (2004b). We confirm their findings that both models fit these data equally well.

We suggest that the best place on the sky to differentiate these two models is towards the Galactic bulge and at low galactic latitudes; we propose that future efforts concentrate on the more challenging task of recovering clean samples of halo FHB stars at low galactic latitudes.

ACKNOWLEDGEMENTS

We thank the UKST staff for their support during the observations. We also thank Lee Clewley and collaborators, who kindly provided the Sersic profile fitting code.

CT would like to thank Tuorla Observatory for its support during an extended stay, and Hamburger Sternwarte for support during several visits. CF thanks the Academy

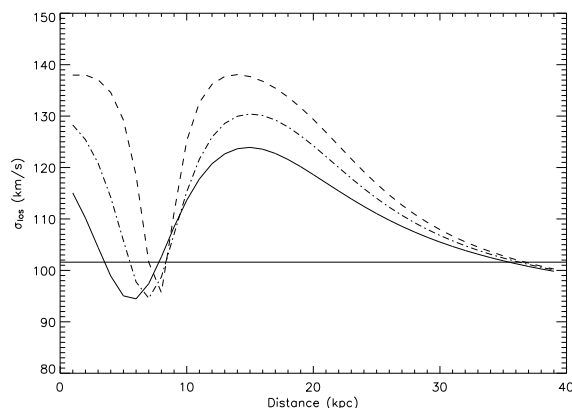


Figure 7. Difference between the SLFC and isothermal model predictions in the direction of the Galactic centre. Dashed, dot-dashed and solid curves are drawn for lines-of-sight at $(l, b) = (0, 15), (0, 30), (0, 45)$ respectively. For comparison, the solid line shows the constant velocity dispersion measured in the Sirko sample.

of Finland and the ANTARES program for its support of space based research. BKG, CF, and CT acknowledge the financial support of the Australian Research Council and its Discovery and Linkage International programs.

T.C.B. acknowledges partial support from grants AST 00-98508, AST 00-98549, and AST 04-06784, as well as from grant PHY 02-16783; Physics Frontier Center/Joint Institute for Nuclear Astrophysics (JINA), awarded by the U.S. National Science Foundation. We are also grateful to Michigan State University for providing partial financial support for the UK Schmidt Telescope during the time the data presented herein were gathered.

REFERENCES

- Beers T. C., Chiba M., Sakamoto T., Wilhelm R., Alende Prieto C., Sommer-Larsen J., Newberg H. J., Yanny B., Marsteller B., Pier J. R., 2004, in IAU Symposium The Mass of the Galaxy from Large Samples of Field Horizontal-Branch Stars in the SDSS Early Data Release. p. 195
- Beers T. C., Preston G. W., Shectman S. A., 1985, *AJ*, 90, 2089
- Beers T. C., Preston G. W., Shectman S. A., 1988, *ApJS*, 67, 461
- Beers T. C., Preston G. W., Shectman S. A., 1992, *AJ*, 103, 1987
- Beers T. C., Wilhelm R., Doinidis S. P., Mattson C. J., 1996, *ApJS*, 103, 433
- Binney J., Tremaine S., 1987, *Galactic dynamics*. Princeton, NJ, Princeton University Press, 1987, 747 p.
- Brown W. R., Geller M. J., Kenyon S. J., Beers T. C., Kurtz M. J., Roll J. B., 2004, *AJ*, 127, 1555
- Chiba M., Beers T. C., 2000, *AJ*, 119, 2843
- Christlieb N., Beers T. C., Thom C., Wilhelm R., Rossi S., Flynn C., Wisotzki L., Reimers D., 2004, *A&A*, in press
- Clewley L., Warren S. J., Hewett P. C., Norris J. E., Evans N. W., 2004, *MNRAS*, 352, 285
- Clewley L., Warren S. J., Hewett P. C., Norris J. E., Peterson R. C., Evans N. W., 2002, *MNRAS*, 337, 87
- Flynn C., Sommer-Larsen J., Christensen P. R., 1996, *MNRAS*, 281, 1027
- Gould A., 2003, *ApJ*, 583, 765
- Gould A., 2004, *ApJ*, 607, 653
- Ibata R. A., Gilmore G., Irwin M. J., 1994, *Nature*, 370, 194
- Kinman T. D., Suntzeff N. B., Kraft R. P., 1994, *AJ*, 108, 1722
- Lynden-Bell D., Lynden-Bell R. M., 1995, *MNRAS*, 275, 429
- Majewski S. R., 1994, *ApJ*, 431, L17
- Morrison H. L., Flynn C., Freeman K. C., 1990, *AJ*, 100, 1191
- Morrison H. L., Mateo M., Olszewski E. W., Harding P., Dohm-Palmer R. C., Freeman K. C., Norris J. E., Morita M., 2000, *AJ*, 119, 2254
- Pearson E., 1926, *Biometrika*, 18, 173
- Perryman M. A. C., 2002, *Ap&SS*, 280, 1
- Preston G. W., Shectman S. A., Beers T. C., 1991, *ApJ*, 375, 121
- Robin A. C., Reylé C., Crézé M., 2000, *A&A*, 359, 103
- Schwarz U. J., Wakker B. P., van Woerden H., 1995, *A&A*, 302, 364
- Sirko E., Goodman J., Knapp G. R., Brinkmann J., Ivezić Ž., Knerr E. J., Schlegel D., Schneider D. P., York D. G., 2004b, *AJ*, 127, 899
- Sirko E., Goodman J., Knapp G. R., Brinkmann J., Ivezić Ž., Knerr E. J., Schlegel D., Schneider D. P., York D. G., 2004a, *AJ*, 127, 914
- Sluis A. P. N., Arnold R. A., 1998, *MNRAS*, 297, 732
- Sommer-Larsen J., Beers T. C., Flynn C., Wilhelm R., Christensen P. R., 1997, *ApJ*, 481, 775
- Sommer-Larsen J., Flynn C., Christensen P. R., 1994, *MNRAS*, 271, 94
- Tippett L., 1925, *Biometrika*, 17, 364
- Wilhelm R., Beers T. C., Gray R. O., 1999, *AJ*, 117, 2308